JOINT INSTITUTE FOR NUCLEAR RESEARCH

Frank Laboratory of Neutron Physics

FINAL REPORT ON THE START PROGRAMME

Polymer-doped porous silicon one-dimensional photonic crystal for gamma-ray detection

Supervisor:

Dr. Zaky A. Zaky Ibrahim

Frank Laboratory of Neutron Physics, Joint Institute for Nuclear Research, Dubna, Russia 141980

Student:

Mahmoud A. M. Hussien

Physics Department, Faculty of Science, Assiut University, Assiut 71516, Egypt

Participation period:

March 16 – April 26,
Winter Session 2025

Dubna, 2025

Polymer-doped porous silicon one-dimensional photonic crystal for gamma-ray detection

Abstract

Detecting the amount of radiation dose remains a challenge nowadays. In this report a one-dimensional sequence photonic crystal structure using porous silicon doped with a polymer of polyvinyl alcohol, carbol fuchsin and crystal violet is suggested. The investigation employs MATLAB, utilizing the transfer matrix method to explore the influence of various geometrical and optical parameters, including radiation doses, incident, angel and layer thicknesses, on the sensitivity of the suggested photonic crystal as a sensor. The transmittance of this one-dimensional photonic crystal sensor is analyzed under differing conditions to identify the optimal parameters. The suggested system showed sensitivity of 0.249 nm/Gy for gamma radiation. This detector is characterized by its straightforward design, high monitoring efficiency, and significant potential for gamma radiation detection.

1. Introduction

Over the past decade, photonic band gap structures, which are also known as photonic crystals (PCs), have evolved from an interest in electromagnetic waves to practical applications in microwave and optical technologies [1]. The regular variation of the dielectric material's refractive index (RI) from which the PC is composed results in a forbidden gap, preventing the development of optical modes within a given frequency range [2]. These PCs have a variety of applications, including mirrors in laser cavities, reflecting coatings for lenses, and paints and dyes [3-8]. According to previous studies, there are several methods have been used to create photonic crystals at different length scales, such as holographic lithography [9], layer-by-layer stacking [10], electrochemical etching [11], and low-pressure chemical vapor deposition [12]. The periodicity of the PCs can change in one, two, or all three spatial dimensions. One-dimensional (1D), two-dimensional (2D), and three-dimensional (3D) PCs are the names given to them, respectively. 1D PCs, commonly referred to as multilayer structures, have been extensively researched and documented in the previous literature [13-17]. 1D PCs simply consist of sequential layers of two materials that have different RIs, leading to a refractive index that periodically varies in one direction while remaining uniform in the other two

directions. 2D PCs exhibit variations in the refractive index across 2D, with the third dimension showing no changes. 3D PCs present structures where the RI is altered across all three spatial dimensions. These configurations are illustrated schematically in Figure 1[18].

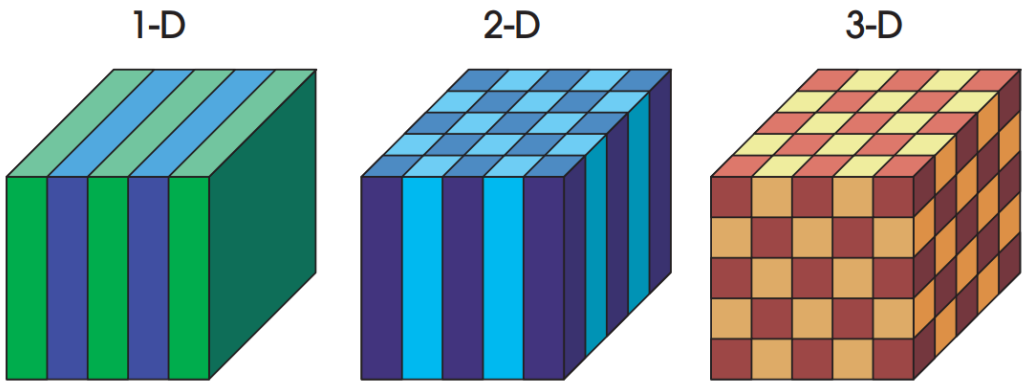

Figure 1 *One dimensional (1D), two-dimensional (2D), and three-dimensional (3D) photonic crystal structure [18].*

In this report we focus on the 1DPCs, which can be fabricated via several methods such as evaporation technique [19], sputtering [19, 20], dip/spin coating [21], anodic etching of crystalline silicon [22], and low-pressure chemical vapor deposition [12]. A variety of applications, including optical sensors, optical switches, optical limiters, temperature sensors, and omnidirectional high reflectors, are enabled by these robust 1DPC structures [23-25]. However, these 1DPCs are promising for colorimetric sensing applications because the theory and sensing mechanisms underlying them are particularly straightforward, which facilitates the prediction of their properties and allows for the rational design to fulfill user requirements [26]. Although all of the aforementioned applications can be performed using pristine PCs, the doped or defective versions may be more beneficial. This is exactly what happens when the properties of semiconductor materials are improved by doping them with certain amounts of specific impurities [27].

Recently, porous silicon (PS) has attracted a lot of interest due to its distinctive optical and luminescent properties [28]. For the creation of photonic band-gap structures, this material is thought to be extremely promising. It is noteworthy that PS displays a wide range of refractive index values. Furthermore, speed, cost-effectiveness, controllability, and compatibility with modern silicon technology are

characteristics of the fabrication process. In 1994, PS multilayers were first shown to function as Bragg reflectors [29]. According to several reviews, these multilayers have been used for a number of purposes, such as the development of color-sensitive photodiodes [30], the control of photoluminescence [31], and the production of liquid sensors [32].

In this report, we build a photonic sensor based on a defected 1DPC using PS doped with a polymer of polyvinyl alcohol, carbol fuchsin and crystal violet (DPV) to measure the patients' dosages of radiation (Gamma radiation) caused by medical diagnostics. The influence rules of geometrical and optical parameters such as the radiation doses, incident angle and thickness of layers are investigated using MATLAB based on the transfer matrix method.

2. Materials and Methods

As shown in Figure 2, by considering a 1DPC built of [Air/$(Po\text{-}Si_1/Po\text{-}Si_2)^N$/ DPV /$(PoSi_1/ PoSi_2)^N$/Substrate] where N indicates the number of periods, $Po\text{-}Si_1$ and $Po\text{-}Si_2$ represent the layers of porous silicon of cavity ratios of 20% and 80%, respectively, and DPV represents the defect layer of polyvinyl alcohol, carbol fuchsin and crystal violet. It is important to mention here that the optical characteristics change in the Z direction. As initial parameters, the thicknesses of layers $PoSi_1$ and $PoSi_2$ are established at $d_1 = 33.7$ nm and $d_2 = 39.5$ nm, respectively, while the thickness of the DPV layer is set as $d_D = d_1 + d_2$ in nm. The refractive indices for air and the substrate are reported as 1 and 1.52, respectively. The values of N and θ are indicated as seven periods and zero, respectively. The structure responding to the incident gamma radiation is investigated by employing the transfer matrix method (TMM) through calculating the s-polarized light (TE) of the incident gamma waves.

The TMM describes the interaction of an incoming electromagnetic wave with a structure using the following matrix:

$$H = \begin{pmatrix} H_{11} & H_{12} \\ H_{21} & H_{22} \end{pmatrix} = (h_1 h_2)^N (h_D)(h_1 h_2)^N \quad (1)$$

where H_{11}, H_{12}, H_{21}, and H_{22} represent the TTM elements while, h_1, h_2 and h_D represent the TMMs of $Po\text{-}Si_1$, $Po\text{-}Si_2$, and the defect layer, respectively. The

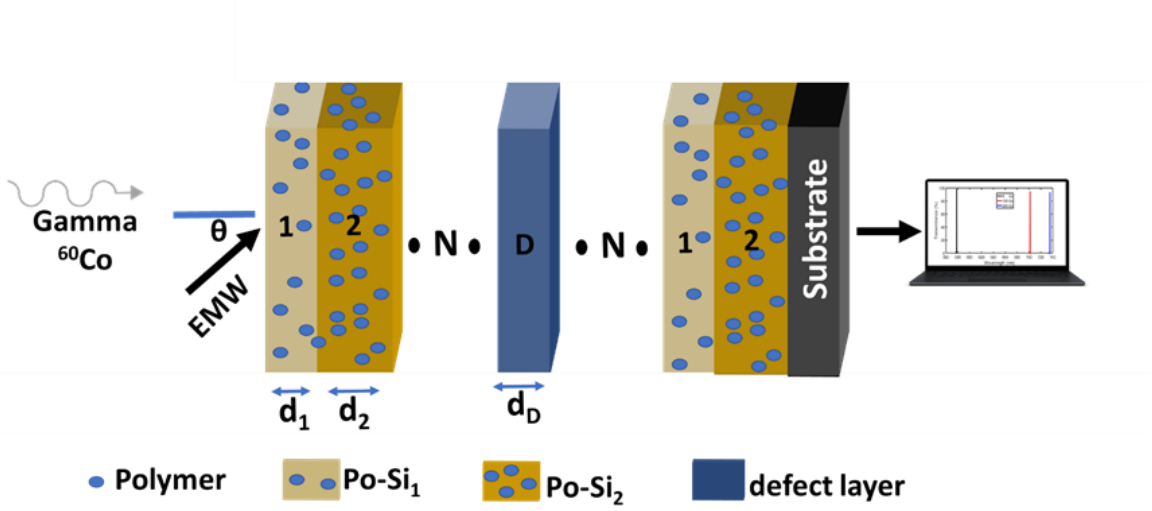

Figure 2 *Schematic structure of the defective 1DPC parodic sequence.*

transmittance spectra (T) of the incident gamma waves can be calculated through the suggested 1DPC given by equation 2 [33]:

$$T(\%) = \frac{p_{air}}{p_{substrate}} \times 100 \times |t^2| \tag{2}$$

where t is the transmittance coefficient and given by:

$$t = \frac{2p_{substrate}}{(H_{11} + H_{12}P_{air})p_{substrate} + (A_{21} + A_{22}p_{air})} \tag{3}$$

where p represents the value of the s-polarization of light at each layer and is given by $p_r = n_r cos\theta_r$. The matrix for each layer can be represented by:

$$h_r = \begin{pmatrix} \cos \emptyset_r & \frac{-i \sin \emptyset_r}{p_r} \\ -ip_r \sin \emptyset_r & \cos \emptyset_r \end{pmatrix} \qquad r = \text{PoSi}_1, \text{PoSi}_2 \text{ and PDV layer} \tag{4}$$

$$\emptyset_r = \frac{2\pi}{\lambda} d_r n_r cos_{\phi_r} \tag{5}$$

Where $\emptyset_r$ is the angel of incidence at each layer, and they obeying Snell's law, λ is the wavelength in nm, n_r is the RI of each layer, and d_r is the thickness of each layer. The effect of gamma radiation doses on the synthesized PDV has been previously studied by Antar using the dipping method [34]. By using Antar's experimental data, the relationship between the RI of the DPV layer and the gamma radiation dose can be fitted [34]. With alterations in radiation doses ranging from 0 Gy to 70 Gy using a ^{60}Co-source, the RI of DPV varies according to the following equation:

$$n_{\_PDV} = C_5\lambda^5 + C_4\lambda^4 + C_3\lambda^3 + C_2\lambda^2 + C_1\lambda^1 + C_0 \quad (6)$$

The coefficients of equation 6 at the different radiation doses are listed in Table 1. Equation 6, which is known as Bruggeman's effective model is utilized to estimate the optical RI constant of Po-Si in terms of the cavities ratio (P), which is filled with DPV [35].

$$n_{Po\_Si} = 0.5\sqrt{\Psi + \sqrt{\Psi^2 + 8n_{Si}^2 n_{DPV}^2}} \quad (7)$$

$$\Psi = 3P\left(n_{PDV}^2 - n_{Si}^2\right) + \left(2n_{Si}^2 - n_{PDV}^2\right)$$

Where Ψ is the and n_{Si} in the refractive index of pure silicon, which can be fitted using the Sellmeir formula (equation 8) from the experimental data collected by Vuye et al. as shown in Figure 3 [36].

$$n_{Si}^2 = 4.92429 + \frac{3.53113\,\lambda^2}{\lambda^2 - 0.34611^2} + \frac{3.52098\,\lambda^2}{\lambda^2 - 0.34610^2} \quad (8)$$

Table 1 The coefficients of the fitted equation of n_{DPV} at the different radiation doses

Dose (Gy)	coefficients
0	$C_5 = -3.5481901\times10^{-11}$ $C_4 = 8.5122412\times10^{-8}$ $C_3 = -8.1190097\times10^{-5}$ $C_2 = 0.03847593$ $C_1 = -9.0594799$ $C_0 = 850.52663$
10	$C_5 = -1.7847077\times10^{-11}$ $C_4 = 4.4209413\times10^{-8}$ $C_3 = -4.3403449\times10^{-5}$ $C_2 = 0.021109774$ $C_1 = -5.0877257$ $C_0 = 488.85561$
20	$C_5 = -1.504232549\times10^{-11}$ $C_4 = 3.725321918\times10^{-8}$ $C_3 = -3.656563575\times10^{-5}$ $C_2 = 0.01777880619$ $C_1 = -4.283140735$ $C_0 = 411.7150827$
30	$C_5 = -1.521210266\times10^{-11}$ $C_4 = 3.753684395\times10^{-8}$ $C_3 = -3.672298445\times10^{-5}$ $C_2 = 0.01780194504$ $C_1 = -4.276873206$ $C_0 = 410.0556432$
40	$C_5 = -1.003069548\times10^{-11}$ $C_4 = 2.496866816\times10^{-8}$ $C_3 = -2.461255088\times10^{-5}$ $C_2 = 0.01200818779$ $C_1 = -2.900587283$ $C_0 = 280.1490142$
50	$C_5 = -1.005931185\times10^{-11}$ $C_4 = 2.5123355\times10^{-8}$ $C_3 = -2.483793981\times10^{-5}$ $C_2 = 0.01215014856$ $C_1 = -2.941970648$ $C_0 = 284.7668504$
60	$C_5 = -7.056381025\times10^{-12}$ $C_4 = 1.792241707\times10^{-8}$ $C_3 = -1.796294415\times10^{-5}$ $C_2 = 0.008884330138$ $C_1 = -2.170145911$ $C_0 = 212.1611348$
70	$C_5 = -5.418362006\times10^{-12}$ $C_4 = 1.396121004\times10^{-8}$ $C_3 = -1.41559553\times10^{-5}$ $C_2 = 0.007067209854$ $C_1 = -1.73936919$ $C_0 = 171.5838239$

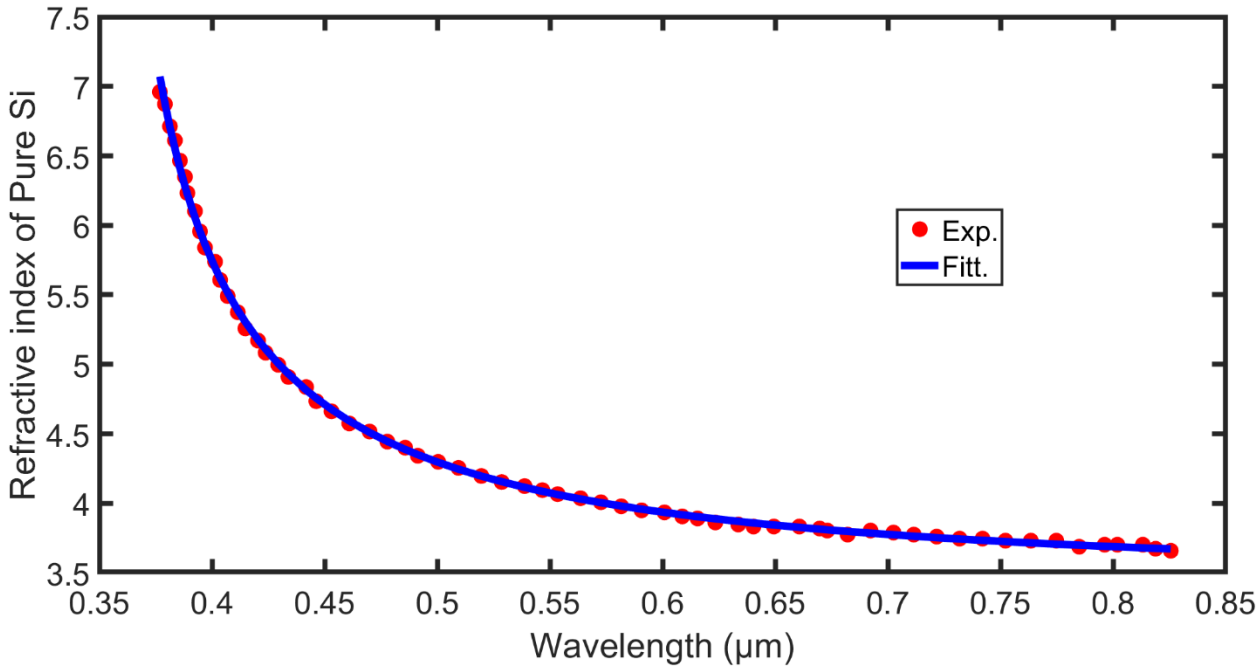

Figure 3 *Experimental [36] and fitted RI (using Eq. 8) of pure Si versus the wavelengths from 0.35 to 0.85 μm.*

Radiation doses have very little effect on silicon's temperature and its RI, with values of less than 3.2ºC and 5×10^{-5}, respectively [37]. Furthermore, Si has a low thermo-optic coefficient (2.3×10^{-4} K^{-1}). As a result, radiation doses have a minor effect on the RI and thickness of Po-Si layers [37].

3. Results and Discussion

Figure 4.a reflects the dependency of the n_{DPV} on λ of the incident electromagnetic wave and the dose of gamma radiation due to the collected data from Antar's work [34]. It is clear that the RI of the DPV almost remains the same in the wavelength range from 390 nm to 450 nm. While, above a wavelength of 450 nm, it exhibits a notable reduction. One can easily note an overlap in the wavelength range from 390 nm to 490 nm, so this range of wavelengths is unsuitable for the detection of gamma doses. The RI of DPV is notably increases by increasing the gamma dose from 0 Gy to 70 Gy over a wavelength range from 490 nm to 550 nm. Figure 4.b displays the refractive indices of Po-Si_1 and Po-Si_2 at different radiation dosages. Over a wavelength range of 490 nm to 550 nm, the RIs of the Po-Si_1 and Po-Si_2 layers exhibit significant variation across various radiation doses.

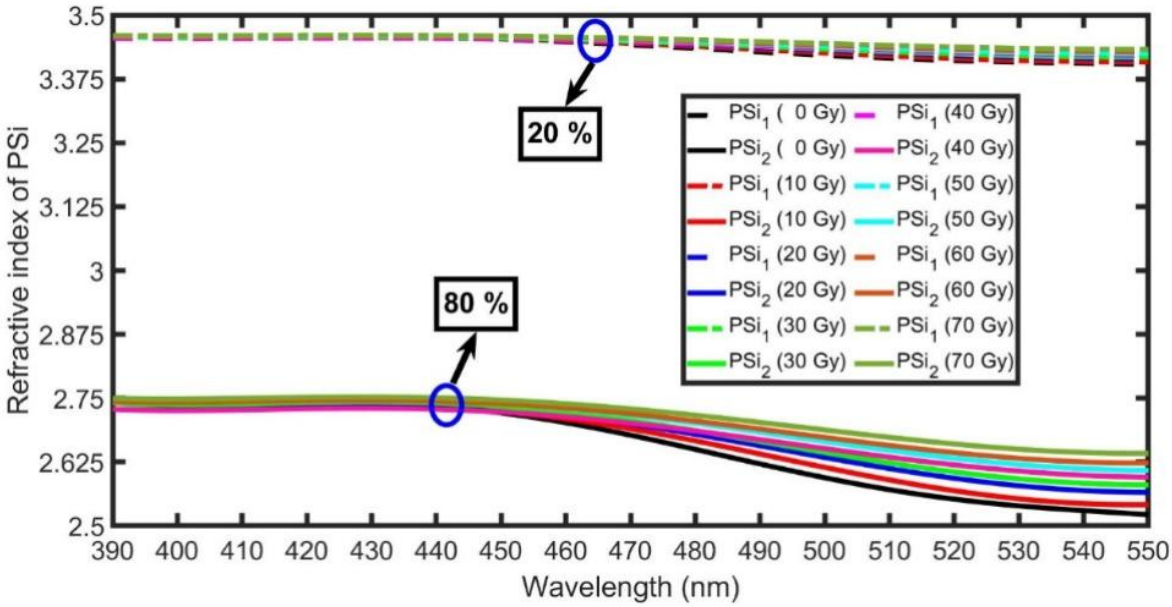

Figure 4.a *Refractive indices of DPV at different Gamma doses in the wavelength range from 390 to 550 nm [38]*

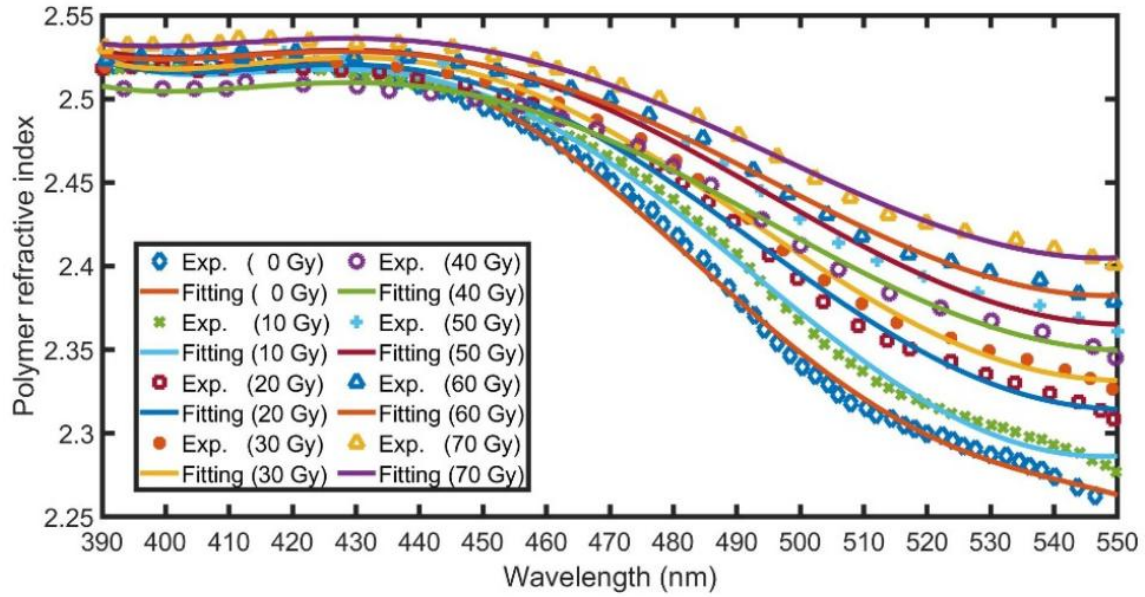

Figure 4.b *Refractive indices Po-Si at different Gamma doses in the wavelength range from 390 to 550 nm [38].*

The transmittances of the suggested defected 1DPC under the aforementioned initial conditions at the different radiation doses of 0, 10, 20, 30, 40, 50, 60 and 70 Gy are demonstrated in Figure 4. It can be noted that the photonic bandgap (PBG) for the 0

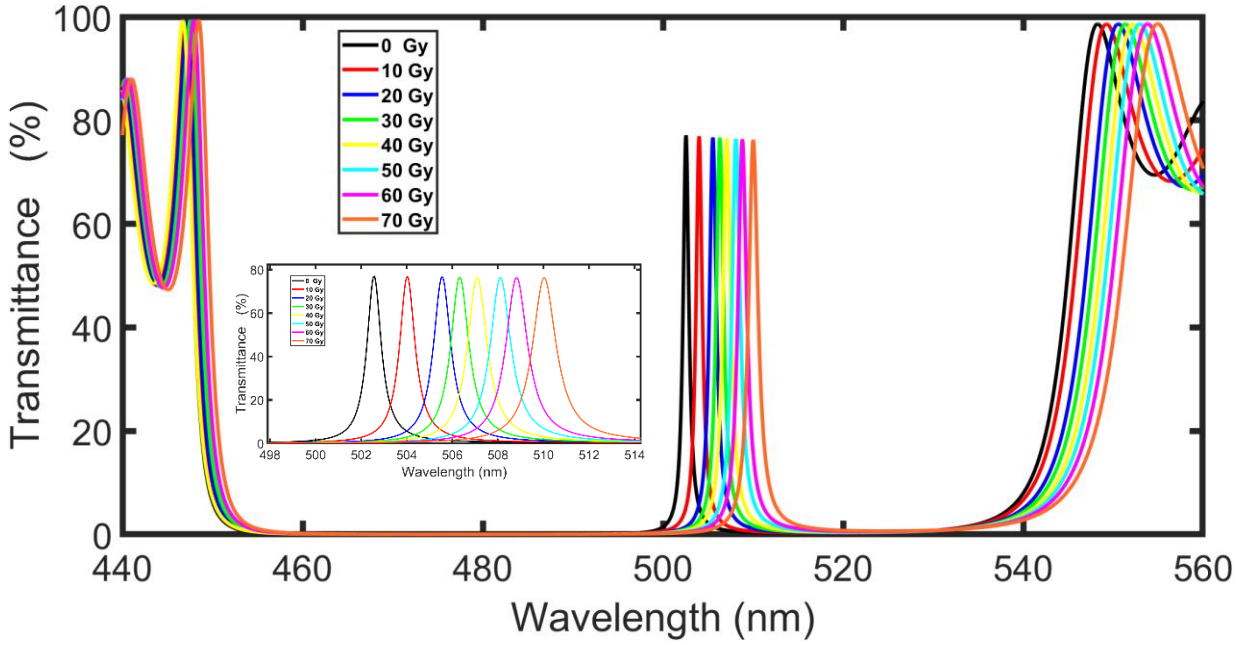

Figure 5 *The transmittances of the proposed 1DPC over the wavelength range from 490 to 550 nm at 0, 10, 20, 30, 40, 50, 60, and 70 Gy of Gamma radiation dose.*

Gy dose broadened from 506 to 532 nm. Increasing the radiation dosage from 0 Gy to 70 Gy causes the PBG to shift towards IR wavelengths. This shift is clearly shown in the inset of Figure 5. The PBG results from the repeated Bragg scattering of the incident EMW [39]. The PBG inhibits the transmission of specific wavelengths within the PC structure [40]. The immersion of the defect layer within the 1DPC is responsible for the appearance of the transmission resonant inside the PBG and the position of this peak is a function of the RI of the defect layer [41].

The sensitivity of the suggested 1DPC as a photonic sensor is a very vital parameter, and it can be determined by the following equation [38]:

$$S(nm/Gy) = \frac{\Delta\lambda}{\Delta\gamma} \tag{9}$$

Where Δλ is the wavelength difference between the position of the resonant peak at 0 Gy and that at any other radiation dose ($\Delta\lambda = \lambda_{radiated} - \lambda_{0Gy}$) and $\Delta\gamma$ is the difference in the radiation dose.

It was observed that the insertion of the defect layer without radiation (0 Gy) resulted in the appearance of a distinct resonant peak at a wavelength of 502.55 nm, accompanied by a high transmission rate of 77%. This peak arises due to the confinement of light within the defect layer. Upon altering the gamma radiation dose

from 10 up to 70 Gy, the resonant peak shifted to a higher wavelength of 510.02 nm, reflecting a wavelength shift of $\Delta\lambda = 7.47$ nm. While $\Delta\lambda$ is equal to 1.64, 2.99, 3.77, 4.54, 5.56, and 6.26 for 10, 20, 30, 40, 50, and 60 Gy of gamma radiation dose, respectively. At 550 nm the RI of the defect layer is 2.26 at 0 Gy and equal to 2.40 at 70 Gy, as indicated experimentally by Antar [34]. The sensitivity calculated from these results is 0.1066 nm/Gy, as determined by equation 9.

3.1 Effect of the DPV layer thickness

In this section the effect of the thickness of the defect layer on the sensitivity for the suggested 1DPC is investigated. As listed in Table 2, the sensitivity increases by increasing the thickness up to 20D (optimal thickness). The resonant peak of the defect experienced a shift of $\Delta\lambda = 16.194$ nm due to the alteration of gamma radiation dose from 0 to 70 Gy. This change corresponds to a maximum sensitivity of 0.23135 nm/Gy. Figures 6a-6d show the dependency of the resonant peak position at 0 Gy, 10 Gy, 20 Gy, 30 Gy, 40 Gy, 50 Gy, 60 Gy, and 70 Gy on the thickness of the defect layer for 5D, 10D, and 15D, where $D = d_1 + d_2$. It is important to note that the sensitivity did not exhibit further increase at greater thickness levels when compared to 15D. Figure 7 provides confirmation of the results in Table 2.

3.2 Effect of the incident angle

The transmittance spectra at 0º, 30º, and 60º incident angles of the EMW were also investigated. As illustrated in Figures 8a-8c, an increase in the incident angle resulted in a rise in the sensor sensitivity. Table 3 presents the enhancement in sensitivity associated with varying incident angles, specifically at a defect layer thickness of 15D. Notably, the sensitivity increased from 0.1691 nm/Gy to 0.2068 nm/Gy as the incident angle shifted from 0° to 60°. It is evident that sensitivity does not exhibit a significant increase at angles greater than 60°. Consequently, an incident angle of 60° is deemed optimal for our sensor.

Table 2 Dependency of the sensitivity on the thickness of the defect layer in the case.

d_D (nm)	$\Delta\lambda$ (nm)	S(nm/Gy)
1D	7.465	0.1066
5D	9.942	0.14203
10D	14.163	0.20233
15D	16.194	0.23135

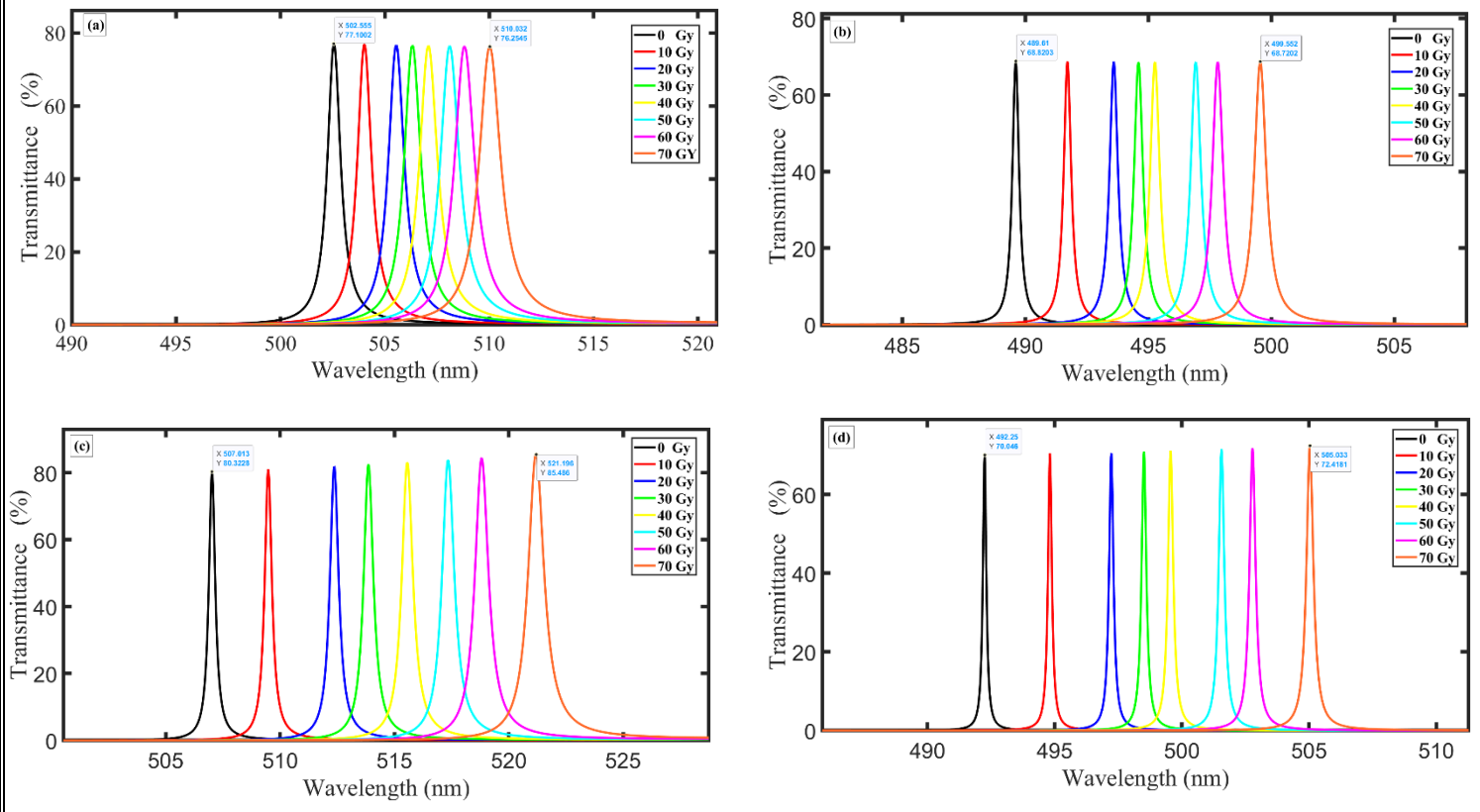

Figure 6 *The transmittances of the suggested 1DPC at a radiation dose of 0 Gy, 10 Gy, 20 Gy, 30 Gy, 40 Gy, 50 Gy, 60 Gy, and 70 Gy versus the thickness of the DPV defect layer at (a) d_D = 1D, (b) d_D = 5D, (c) d_D = 10D, and (d) d_D = 15D.*

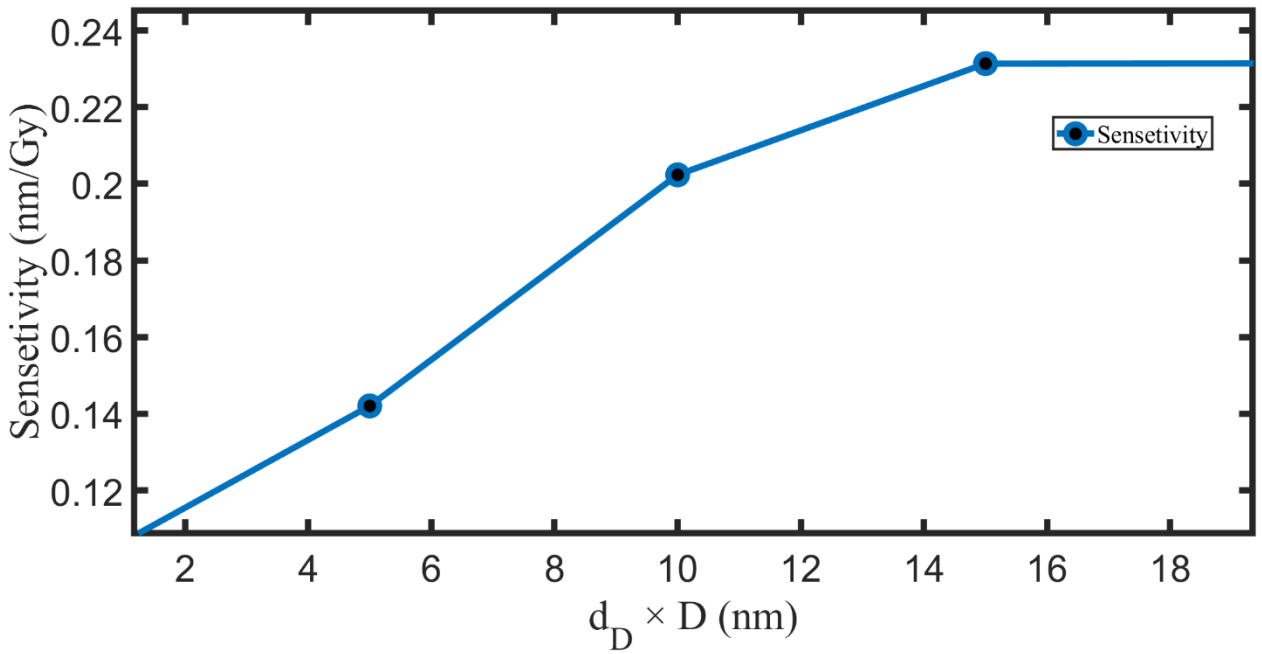

Figure 7 *The sensitivity of the proposed structure versus the thickness of the DPV defect layer.*

Table 3 Dependency of the sensitivity on the EMW incident angel for d_D = 15D.

θ (Dgree)	Δλ (nm)	S(nm/Gy)
0	11.156	0.1593
30	12.783	0.1826
60	14.479	0.2068

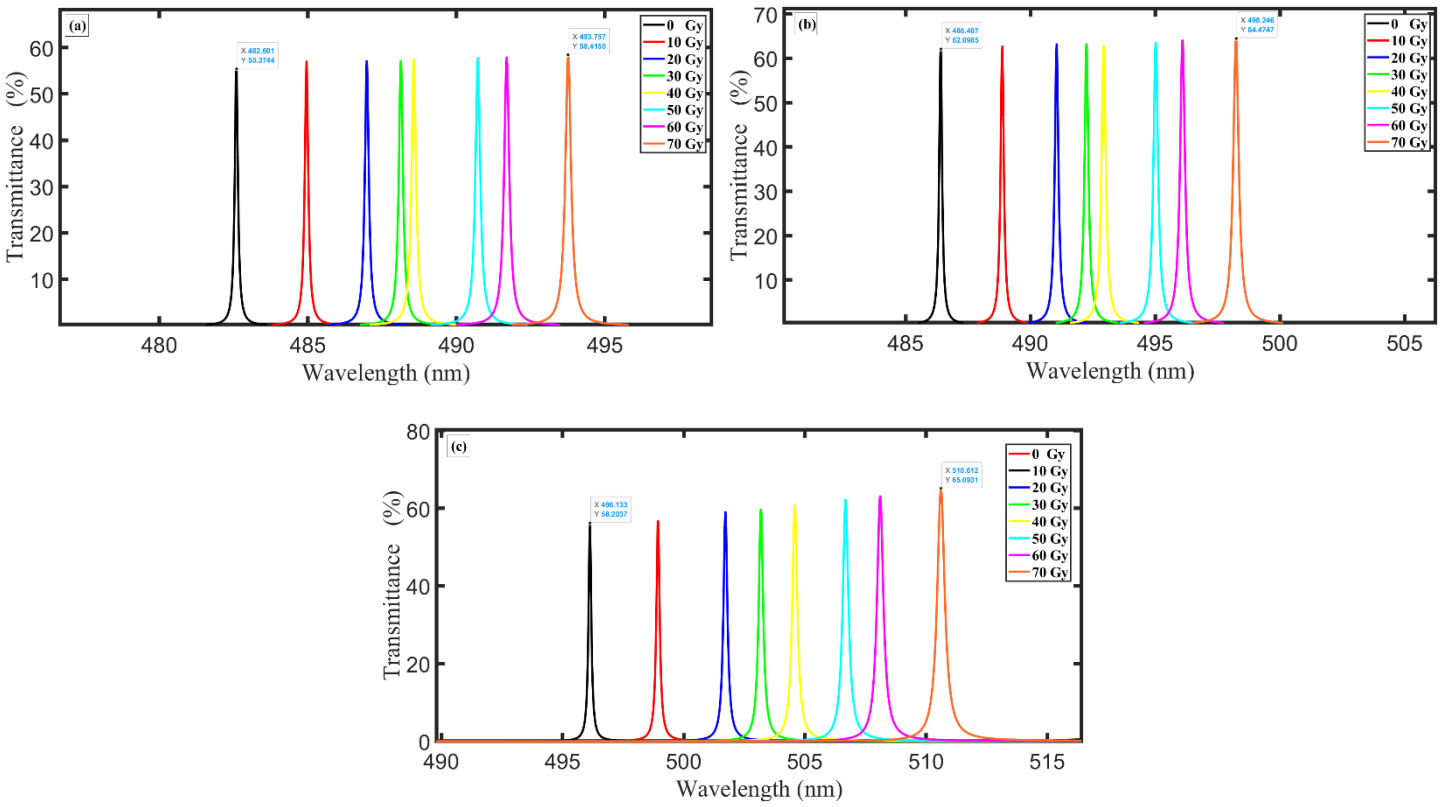

Figure 8 *The transmittances of the suggested 1DPC at a radiation dose of 0 Gy, 10 Gy, 20 Gy, 30 Gy, 40 Gy, 50 Gy, 60 Gy, and 70 Gy versus the thickness of the incident angel of the EMW (a) θ = 0°, (b) θ = 30°, and (c) θ = 60°.*

4. Conclusion

1DPC structure was proposed as a gamma radiation dose detector. Two Po-Si layers doped with DPV and a defect layer of DPV were able to create a periodic structure with PBG and defect peak. The porosity and geometry of the structure are optimized to evaluate the system's functioning. With changing the radiation doses from 0 Gy, 10 Gy, 20 Gy, 30 Gy, 40 Gy, 50 Gy, 60 Gy and 70 Gy, the resonant peaks were at 524.71 nm, 526.98 nm, 530.94 nm, 533.15 nm, 535.77 nm, 537.95 nm,

540.27 nm and 543.71 nm with a transmittance of 82%, respectively. The proposed system recorded the accepted sensitivity of 0.23135 nm/Gy for gamma radiation.

References

[1] Krauss T F and Richard M 1999 Photonic crystals in the optical regime—past, present and future *Progress in Quantum electronics* **23** 51-96

[2] Ge J and Yin Y 2011 Responsive photonic crystals *Angewandte Chemie International Edition* **50** 1492-522

[3] John S 1987 Strong localization of photons in certain disordered dielectric superlattices *Physical review letters* **58** 2486

[4] Yablonovitch E 1987 Inhibited spontaneous emission in solid-state physics and electronics *Physical review letters* **58** 2059

[5] Yablonovitch E 2001 Photonic crystals: semiconductors of light *Scientific American* **285** 46-55

[6] Krauss T F 2003 Cavities without leaks *Nature Materials* **2** 777-8

[7] Akahane Y, Asano T, Song B-S and Noda S 2003 High-Q photonic nanocavity in a two-dimensional photonic crystal *nature* **425** 944-7

[8] Norris D J 2007 A view of the future *Nature Materials* **6** 177-8

[9] Campbell M, Sharp D, Harrison M, Denning R and Turberfield A 2000 Fabrication of photonic crystals for the visible spectrum by holographic lithography *nature* **404** 53-6

[10] Lin S-y, Fleming J, Hetherington D, Smith B, Biswas R, Ho K, Sigalas M, Zubrzycki W, Kurtz S and Bur J 1998 A three-dimensional photonic crystal operating at infrared wavelengths *nature* **394** 251-3

[11] Birner A, Wehrspohn R B, Gösele U M and Busch K 2001 Silicon-based photonic crystals *Advanced Materials* **13** 377-88

[12] Patrini M, Galli M, Belotti M, Andreani L, Guizzetti G, Pucker G, Lui A, Bellutti P and Pavesi L 2002 Optical response of one-dimensional (Si/SiO 2) m photonic crystals *Journal of applied physics* **92** 1816-20

[13] Centini M, Sibilia C, Scalora M, D'aguanno G, Bertolotti M, Bloemer M, Bowden C and Nefedov I 1999 Dispersive properties of finite, one-dimensional photonic band gap structures: applications to nonlinear quadratic interactions *Physical Review E* **60** 4891

[14] Lidorikis E, Li Q and Soukoulis C M 1996 Wave propagation in nonlinear multilayer structures *Physical Review B* **54** 10249

[15] Moussa R, Salomon L, Dufour J and Aourag H 2002 Large photonic band gap's in one-dimensional multilayer structures *Journal of Physics and Chemistry of Solids* **63** 725-32

[16] Kavokin A, Malpuech G, Di Carlo A, Lugli P and Rossi F 2000 Photonic Bloch oscillations in laterally confined Bragg mirrors *Physical Review B* **61** 4413
[17] Inouye H, Arakawa M, Ye J Y, Hattori T, Nakatsuka H and Hirao K 2002 Optical properties of a total-reflection-type one-dimensional photonic crystal *IEEE Journal of quantum electronics* **38** 867-71
[18] Joannopoulos J, Meade R D and Winn J 1995 Photonic Crystals–Princeton *Princeton, NJ*
[19] Bloemer M J and Scalora M 1998 Transmissive properties of Ag/MgF 2 photonic band gaps *Applied Physics Letters* **72** 1676-8
[20] Lee H-Y, Makino H, Yao T and Tanaka A 2002 Si-based omnidirectional reflector and transmission filter optimized at a wavelength of 1.55 μm *Applied Physics Letters* **81** 4502-4
[21] Bellessa J, Rabaste S, Plenet J, Dumas J, Mugnier J and Marty O 2001 Eu 3+-doped microcavities fabricated by sol–gel process *Applied Physics Letters* **79** 2142-4
[22] Nair R V and Vijaya R 2010 Photonic crystal sensors: An overview *Progress in Quantum electronics* **34** 89-134
[23] Sun Y-P, Riggs J E and Liu B 1997 Optical limiting properties of [60] fullerene derivatives *Chemistry of materials* **9** 1268-72
[24] Tran P 1996 Optical switching with a nonlinear photonic crystal: a numerical study *Optics Letters* **21** 1138-40
[25] Ali N B, Alsaif H, Trabelsi Y, Chughtai M T, Dhasarathan V and Kanzari M 2021 High sensitivity to salinity-temperature using one-dimensional deformed photonic crystal *Coatings* **11** 713
[26] Däntl M, Jiménez-Solano A and Lotsch B V 2022 Stimuli-responsive one-dimensional photonic crystals: design, fabrication and sensing *Materials Advances* **3** 7406-24
[27] Aly A H and Elsayed H A 2012 Defect mode properties in a one-dimensional photonic crystal *Physica B: Condensed Matter* **407** 120-5
[28] Cullis A, Canham L T and Calcott P 1997 The structural and luminescence properties of porous silicon *Journal of applied physics* **82** 909-65
[29] Vincent G 1994 Optical properties of porous silicon superlattices *Applied Physics Letters* **64** 2367-9
[30] Krüger M, Berger M G, Marso M, Reetz W, Eickhoff T, Loo R, Vescan L, Thönissen M, Lüth H and Arens-Fischer R 1997 Color-sensitive Si-photodiode using porous silicon interference filters *Japanese journal of applied physics* **36** L24

[31] Cazzanelli M, Vinegoni C and Pavesi L 1999 Temperature dependence of the photoluminescence of all-porous-silicon optical microcavities *Journal of applied physics* **85** 1760-4
[32] Zangooie S, Jansson R and Arwin H 1998 Reversible and irreversible control of optical properties of porous silicon superlattices by thermal oxidation, vapor adsorption, and liquid penetration *Journal of Vacuum Science & Technology A: Vacuum, Surfaces, and Films* **16** 2901-12
[33] Yeh P and Hendry M 1990 Optical waves in layered media. American Institute of Physics)
[34] Antar E 2014 Effect of γ-ray on optical characteristics of dyed PVA films *Journal of Radiation Research and Applied Sciences* **7** 129-34
[35] Zaky Z A, Alamri S, Zhaketov V and Aly A H 2022 Refractive index sensor with magnified resonant signal *Scientific Reports* **12** 13777
[36] Vuye G, Fisson S, Van V N, Wang Y, Rivory J and Abeles F 1993 Temperature dependence of the dielectric function of silicon using in situ spectroscopic ellipsometry *Thin Solid Films* **233** 166-70
[37] Du Q, Huang Y, Ogbuu O, Zhang W, Li J, Singh V, Agarwal A M and Hu J 2017 Gamma radiation effects in amorphous silicon and silicon nitride photonic devices *Optics Letters* **42** 587-90
[38] Zaky Z A, Al-Dossari M, Hendy A S, Zayed M and Aly A H 2024 Gamma radiation detector using Cantor quasi-periodic photonic crystal based on porous silicon doped with polymer *International Journal of Modern Physics B* **38** 2450409
[39] Taya S A and Shaheen S A 2018 Binary photonic crystal for refractometric applications (TE case) *Indian Journal of Physics* **92** 519-27
[40] Aly A H, Ryu S-W and Wu C-J 2008 Electromagnetic wave propagation characteristics in a one-dimensional metallic photonic crystal *Journal of Nonlinear Optical Physics & Materials* **17** 255-64
[41] Aly A H and Mohamed D 2015 BSCCO/SrTiO 3 one dimensional superconducting photonic crystal for many applications *Journal of Superconductivity and Novel Magnetism* **28** 1699-703